Rate of Solution of Solid Particles in Agitated Liquids

By

Shinji NAGATA, Masaaki ADACHI and Iwao YAMAGUCHI

(Received November 30, 1957)

Abstract

Hixson and Baum have proposed generalized dimensionless equations for the rate of solution of solid particles in agitated liquids. The authors developed an improved equation and conducted additional experiments on the rates of solution of zinc and magnesium metals in dilute hydrochloric acid containing potassium nitrate. Experiments were also made on the rate of solution of benzoic acid in NaOH solutions and of sugar in water. The newly developed equation is as follows:

$$\left(\frac{KD}{D_f}\right) = \alpha'\left(\frac{D^2 n \rho_l}{\mu}\right)^p \left(\frac{\mu}{\rho_l D_f}\right)^q \left(\frac{\delta^3 g}{\nu^2}\right)^r \left(\frac{\delta}{D}\right)^s \left(\frac{\rho_s - \rho_l}{\rho_l}\right)^t$$

The constant α' and exponents p, q and s are presented in this paper.

The authors arrived at the following conclusions:

(1) At a definite critical Reynolds number, R_f (or agitator speed, N_f), solid particles are fluidized in an agitated liquid.

(2) At this critical Reynolds number (or agitator speed), the rate of increase in solution velocity is abruptly decreased with further increase in agitator speed.

(3) In the fluidized state where $N > N_f$, an increase in density difference between the solid and liquid phases combined with the effect of agitation velocity greatly reduces the diffusional resistance.

(4) In the range of Reynolds numbers less than R_f, or agitator speed less than N_f, the apparent rate of solution of solid particles increases with the 1.0 to 1.4 power of R_e depending upon the conditions of agitation. This experimental effect may reach a value of even 2.9 for small particles.

(5) From these experiments it is expected that the effect of agitation in liquid-liquid systems is mainly to increase the reaction surface area, and that the effect of agitation in diminishing diffusion resistance is rather small. The effect of agitation in solid-liquid systems in the range of fluidization is mainly to diminish diffusional resistance.

1. Experiments of Hixson and Baum[1)]

Hixson and Baum made pioneering studies on the rate of solution of solid particles in agitated liquids. They derived generalized dimensionless equations relating the rate of solution of benzoic acid, sodium chloride and barium chloride in water and in other solvents. They studied the effect of the following factors upon the solution rate coefficient K (cm/sec) and on the thickness of the diffusion film x (cm).

(1) agitator speed in r.p.s., n (1/sec)
(2) diameter of agitation vessel, D (cm)
(3) density of liquid, ρ_l (g/cm^3)
(4) viscosity of liquid, μ (g/cm·sec)
(5) diffusion coefficient of solute, D_f (cm^2/sec)

The following dimensionless equation was derived:

$$\left(\frac{KD}{D_f}\right) = \frac{D}{x} = f_1\left(\frac{D^2 n \rho_l}{\mu}\right) \cdot f_2\left(\frac{\mu}{\rho_l D_f}\right) \tag{1}$$

or

$$\left(\frac{KD}{D_f}\right) = \frac{D}{x} = \alpha\left(\frac{D^2 n \rho_l}{\mu}\right)^p \left(\frac{\mu}{\rho_l D_f}\right)^q \tag{1'}$$

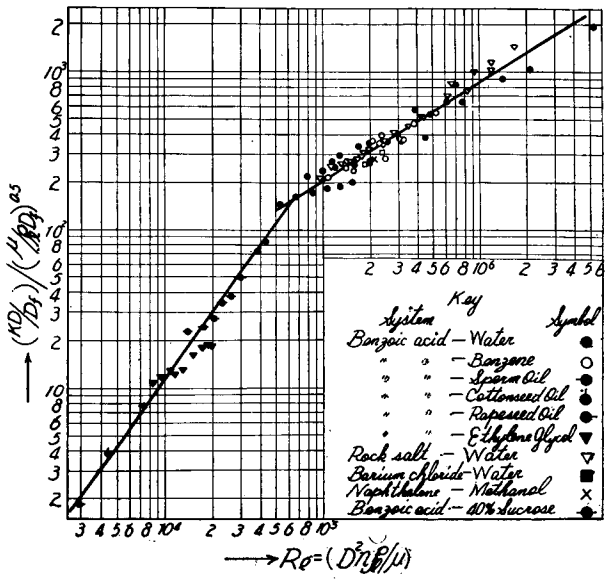

Fig. 1. General correlation of data by Hixson and Baum.

Hixson and Baum experimented with vessels of different dimensions in evaluating the coefficients and exponents of Eq. (1'). The results of their studies are shown in **Fig. 1.** The correlations of $(KD/D_f)/(\mu/\rho_l D_f)^{0.5}$ vs $(D^2 n \rho_l/\mu)$ are represented by straight lines on logarithmic paper.

For values of $R_e > 6.7 \times 10^4$, where $R_e = D^2 n \rho_l / \mu$.

$$\left(\frac{KD}{D_f}\right) = \frac{D}{x} = 0.16\left(\frac{D^2 n \rho_l}{\mu}\right)^{0.62}\left(\frac{\mu}{\rho_l D_f}\right)^{0.5} \tag{2}$$

For values of $R_e < 6.7 \times 10^4$,

$$\left(\frac{KD}{D_f}\right) = \frac{D}{x} = 2.7 \times 10^{-5}\left(\frac{D^2 n \rho_l}{\mu}\right)^{1.4}\left(\frac{\mu}{\rho_l D_f}\right)^{0.5} \tag{3}$$

The critical Reynolds number (6.7×10^4) is designated by R_f and corresponds to the Reynolds number at which the solid particles are fluidized.

2. Revision of the Rate Equation of Hixson and Baum.

Upon re-examination of the results of Hixson and Baum, the authors found an inconsistency. In the range of values of R_e greater than R_f, the scattering of data as shown in **Fig. 1** is by no means random. Systematic deviations of the plotted points occur corresponding to different vessel diameters. The data of the benzoic acid-water system were replotted on a larger scale as shown in **Fig. 2.** The data corresponding to the separate parameter of D, 15.2, 20.6, 26.0, 45.7 and 61.0 cm, face on parallel lines. The slope of these lines (the exponents of R_e), are all equal to 0.2

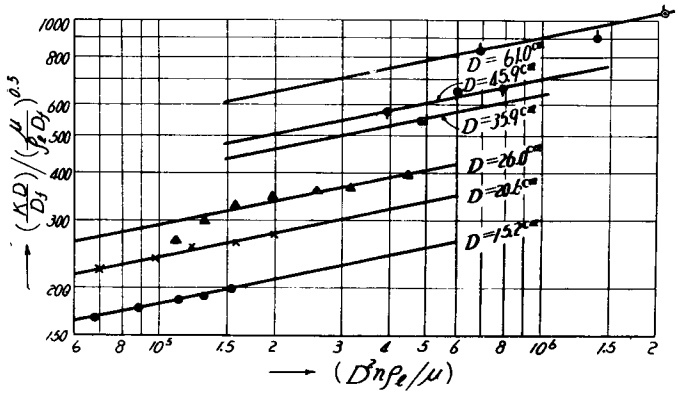

Fig. 2. Benzoic acid-water system by Hixson and Baum.

and not 0.62 as reported by Hixson and Baum in Eq. (2). This behavior also occurred in other systems, but with higher exponents depending upon the density of the solid. For example, in sodium chloride-water system, the exponent of R_e is 0.54, and in the barium chloride-water system, 0.67. It is evident that the exponent of R_e is affected by difference in densities between the solid particles and the liquid phase.

Hixson, *et al.* overlooked the effect of particle size δ (cm), particle shape and particle density ρ_s (g/cm^3). Dimensional analysis is made of eight factors not including particle shape with the following result:

$$\left(\frac{KD}{D_f}\right) = \frac{D}{x} = \alpha'\left(\frac{D^2 n\rho_l}{\mu}\right)^p \left(\frac{\mu}{\rho_l D_f}\right)^q \left(\frac{\delta^3 g}{\nu^2}\right)^r \left(\frac{\delta}{D}\right)^s \left(\frac{\rho_s - \rho_l}{\rho_l}\right)^t \qquad (4)$$

where ν $(=\mu/\rho_l)$ is the kinematic viscosity of the liquid.

As shown by **Fig. 2,** the relation between $\log[(KD/D_f)/(\mu/\rho_l D_f)^{0.5}]$ vs $\log R_e$ is linear. All the experimental data for a vessel of given diameter lie on the same straight line, and the data obtained with vessels of different diameters fall on different lines. The plots of $\log[(KD/D_f)/(\mu/\rho_l D_f)^{0.5} R_e^{0.2}]$ vs $\log(\delta/D)$ give a value of 0.8 for the exponents of Eq. (4). A plot of $\log[(KD/D_f)/(\mu/\rho_l D_f)^{0.5}(\delta/D)^{-0.8}]$ vs $\log R_e$ gives a straight line as shown by curve (1) in **Fig. 3** with the exponent (p) for R_e

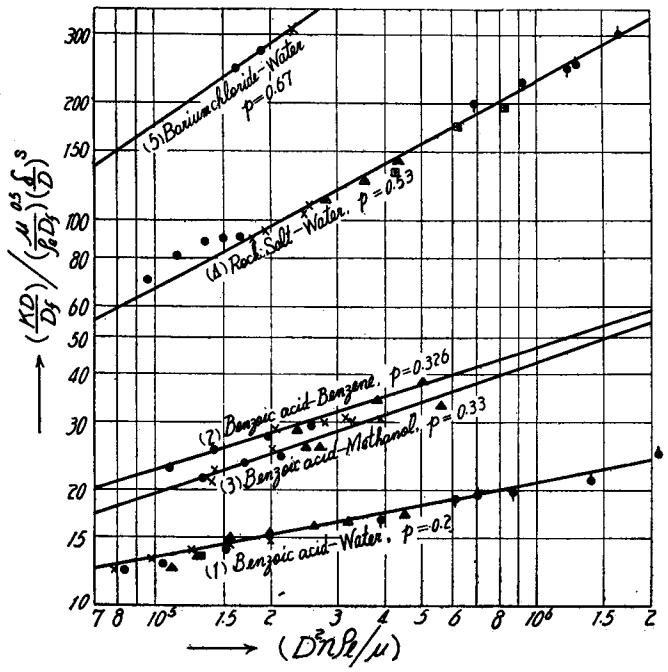

Fig. 3. Revised correlation of (KD/D_f) vs $(D^2 n\rho_l/\mu)$.

equal to 0.20 for the benzoic acid-water system. Thus for the benzoic acid-water system the following equation is obtained:

$$\left(\frac{KD}{D_f}\right) = \frac{D}{x} = \alpha''\left(\frac{D^2 n\rho_l}{\mu}\right)^{0.2} \left(\frac{\mu}{\rho_l D_f}\right)^{0.5} \left(\frac{\delta}{D}\right)^{-0.8} \qquad (5)$$

For other systems, similar equations were obtained with values of exponents tabulated in **Table 1.**

From **Table 1,** it is clear that with increasing values of $(\rho_s - \rho_l)$ the exponent p increases. In other words an increase in the density difference has a marked effect in reducing diffusional resistance.

For range of Reynolds number less than R_f, solid particles gather beneath the impeller as shown by **Fig. 6a.** The solid surface confined within the pile of particles is not readily available for dissociation. With an increase in agitator speed, the effective surface area is gradually increased. This accounts for the high exponent 1.4 of R_e in this velocity range.

Table 1. Exponents of Eq. (4)

System	Density difference $\rho_s - \rho_l$	p_2	s
Benzoic acid-water	0.266	0.20	0.80
Benzoic acid-benzene	0.388	0.326	0.69
Benzoic acid-methanol	0.474	0.333	0.60
Sodium chloride (Rock salt)-water	1.17	0.53	0.32
Barium chloride-water	2.10	0.67	—

Thus it appears that not only the diffusion resistance but also the availability of the surface area vary with change in agitator speed. Hixson, *et al.* derived Eq. (3) on the basis that the surface area of solid particles was proportional to the 2/3 power of the mass of solid, however they neglected the reduced availability of this surface in the region below R_f. As mentioned later, this exponent p_1 also varies with the conditions of agitation, particle size, and density.

3. Rate of Dissolution of Benzoic Acid.

As a result of an examination of Hixson's data, the following results were observed:
(1) At a definite critical Reynolds number R_f, the rate of increase in solution velocity with the increase in agitator speed is abruptly reduced.
(2) The rate of solution increases with the 1.4 power of agitator speed at values below R_f. In this range the particles pile beneath the impeller.
(3) In the fluidization range ($R_e > R_f$), the favorable effect of agitation in reducing diffusional resistance is further increased by increased differences in densities between the phases.

Although these three effects seem evident, the authors verified them with additional precise measurements.

a) Experimental Procedure.

The experimental procedure adopted was almost the same as that used by Mack, *et al.*[2]. Dilute NaOH solution of a certain concentration was used with phenolphthalein as an indicator. After a steady state of agitation was reached, a definite quantity of benzoic acid was added. The tablets were 4 mm in diameter, 2.8 mm in thickness and weighed about 0.04 gr each. The time (θ_0) required for complete neutralization

was observed. It was necessary in these experiments that the concentration of alkaline solution and the number of benzoic acid tablets added were controlled so that the color change could be easily recognized, and the decrease in the size of benzoic acid tablets made neglibible. In the experiments of Part I NaOH solution of 5×10^{-4} normality was used and 200 benzoic acid tablets were added to 3 liters of solution.

b) Rate of Solution.

The concentration gradient in the diffusion film where the neutralization reaction occurs between benzoic acid and NaOH, is shown in **Fig. 4.** It is assumed that the neutralization reaction occurs instantaneously on the plane I–I where equimolal diffusion of benzoic acid and NaOH occurs.

The solution rate of benzoic acid $(dW/d\theta)$ at any instant is expressed as follows:

$$\frac{dW}{d\theta} = \frac{D_B}{x_1} S(c_s - 0) \qquad (6)$$

where

W = moles of benzoic acid dissolved.

θ = time elapsed in the contact of benzoic acid with NaOH solution.

S = total surface area of solid particles.

D_B = diffusion coefficient of benzoic acid in the solution.

x_1 = thickness of the diffusion layer from the surface of solid to the plane where neutralization reaction takes place (**Fig. 4**). The value of x_1 changes with lapse of time.

c_s = concentration of benzoic acid at saturation.

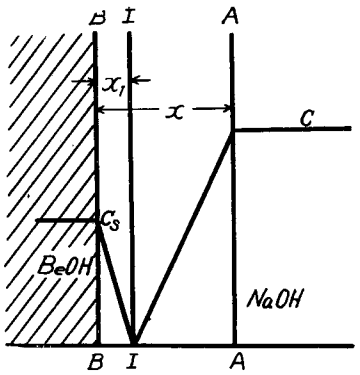

Fig. 4. Diagram showing the concentration gradients in diffusion film.

If the assumption is correct that the neutralization reaction occurs instantaneously, then the concentrations of both solutes may be taken as zero at plane (I–I), then the following relation is derived:

$$\frac{dW}{S\cdot d\theta} = \frac{D_B\cdot c_s}{x_1} = \frac{D_A\cdot c}{x-x_1} \qquad (7)$$

where

c = concentration of alkali at time θ.

D_A = diffusion coefficient of NaOH.

x = thickness of diffusion film.

Since the moles of benzoic acid dissolved, W, are equal to

$V(c_0-c)$, Eq. (6) may be rewritten as follows:

$$-\frac{Vdc}{d\theta}=\frac{D_B}{x_1}S\cdot c_s$$

where V=total volume of alkaline solution.
Substituting x_1 from Eq. (7),

$$-\frac{Vdc}{d\theta}=\frac{(c_sD_B+cD_A)\,S}{x} \tag{8}$$

Integration of Eq. (8) and substitution of $c=c_0$ at $\theta=0$ give the following relation:

$$\ln\frac{c_sD_B+cD_A}{c_sD_B+c_0D_A}=-\frac{D_A\cdot S}{x\cdot V}\theta \tag{9}$$

In Eq. (9), c_s, c_0, D_A, D_B, S and V are all constant at a given temperature and the value of x decreases with increase in agitator speed. Let $(D_A\cdot S/x\cdot V)=K(S/V)=K'$, where K' is a value proportional to the solution rate coefficient K. The coefficient K' is related to agitator speed and according to Eq. (9), is inversely proportional to the time required for neuralization (θ_0).

In the comparison of lines representing $(1/\theta_0)$ vs N (**Fig. 7**), the slope for values below N_f is designated as p_1 and for values above N_f as p_2, thus in Eq. (2) $p_2=0.62$ and in Eq. (3) $p_1=1.4$.

c) Experimental Equipment.

A cylindrical glass vessel with a flat bottom was used. The liquid depth (H) was always chosen equal to the vessel diameter (D) (**Fig. 5**). The blade angle (θ) is measured relative to the rotation plane. Other experimental conditions were as follows:

Part I : D=154 mm, $d=D/3$, $b=0.06\,D$, $n_p=4$,
direction of rotation; normal and reverse.

Part II: D=100 mm, $d=D/2$,
$b=0.15\,D$, $n_p=4$
direction of rotation;
normal.

Rotation of the impeller to lift the liquid upwards corresponds to normal rotation. The number of impeller blades is designated as n_p. The liquid level, H, corresponding to vessel diameter, D, is designated as $H=10$. Liquid levels corresponding to 10 equal division are marked

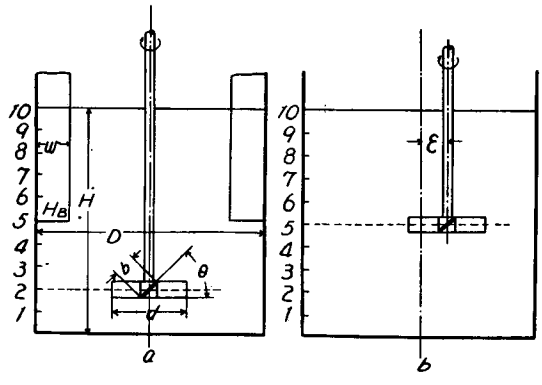

Fig. 5. Diagram showing the condition of agitation.

from the top surface downwards as, 10, 9, ··· 2, 1. For example in **Fig. 5a,** the elevation of the impeller is shown as $H_p=2$ and the elevation of baffle plate as $H_B=5$, The width of the baffle plates, w, was taken as equal to 15% of the vessel diameter and the number of baffles used was 4 and 2, designated as $n_B=4$ and $n_B=2$, respectively. The baffles were always installed symmetrically.

In some cases, the agitator shaft was offset from the center line. The distance from the center line is designated as $\varepsilon=d/4$, $\varepsilon=D/4$ etc. (**Fig. 5b**).

d) Experimental Result, Part I (Effect of Agitation).

Two patterns of flow for the solid particles due to the differences in agitation conditions occur.

(1) When the impeller is lifted from the bottom of the vessel, part of the particles tends to pile up on the bottom below the impeller and part circulates in the liquid around the axis of the agitator. With increase in agitator speed, the solid particles in suspension circulate in a doughnut shape path and when a certain speed is exceeded some of the particles rise above the impeller. However, the main bulk of particles is confined below the rotational plane of the impeller. This pattern of flow is designated as type I as shown in **Fig. 6a.**

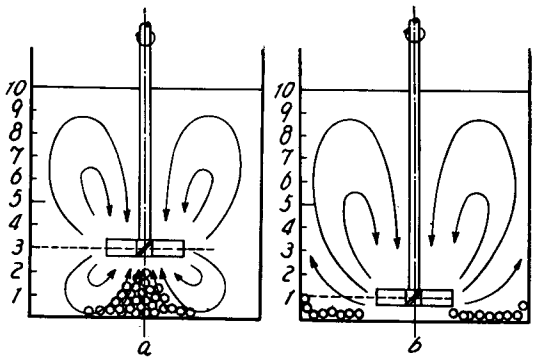

Fig. 6. Diagram showing two types of flow patterns.

(2) When an impeller is located above and near the bottom of the vessel or when the vessel is equipped with baffle plates, solid particles are scattered about the bottom of the vessel and a part of these are moved to the circumference. When the impeller speed is increased, part of the solid particles are thrown into a region above the impeller. This pattern of flow is designated as type II as shown in **Fig. 6b.**

As shown by **Figs. 7, 8** and **9,** the rate of increase in $(1/\theta_0)$ is large until a certain impeller speed is reached, thereafter the rate of increase becomes much less. This critical speed corresponding to the completion of fluidization of solid particles is called the fluidization velocity, N_f. Hereafter, the range of speed below N_f is designated as the stagnant range and the range above N_f as the fluidization range.

Effect of the Impeller Elevation.

In the range of agitator speed less than N_f, the slope of lines $(1/\theta_0)$ vs N is large as shown in **Fig. 7.** Differences occur between the slopes of curve (2′) and (3′)

for impeller blade angle $\theta=45°$ and of curves (1′) and (4′) when $\theta=90°$. The slope at $\theta=45°$ is slightly larger than that at $\theta=90°$. This is because the former belongs to type I where the effective surface area increases with the increase in agitator speed, whereas the latter belongs to type II where the availability of surface area remains nearly constant.

The second characteristic difference between types I and II is that curves of $H_p=3$ show smaller values of N_f and have larger values of $(1/\theta_0)$ for the same agitator speed, compared with curves of $H_p=1$ (Curves for $H_p=5$ and 7 overlap those of $H_p=3$) for the following apparent reasons.

The vertical component of liquid flow is shown by **Fig. 6a** for $H_p=3$ and by **Fig. 6b** for $H_p=1$. The tangential component of liquid flow may be taken to be practically the same. In the case of **Fig. 6a,** solid particles gather in the central part of the vessel where a high density of stream lines occurs, i.e., liquid velocity is large permitting the solid particles to be fluidized at lower agitator speeds. In the case of **Fig. 6b,** solid particles are forced to the circumference of the vessel where the density of stream lines is low and fluidization becomes more difficult. Abnormalities occur below 300 r.p.m. in curves (5′) and (7′) of **Fig. 7** due to transition of flow from type I to II.

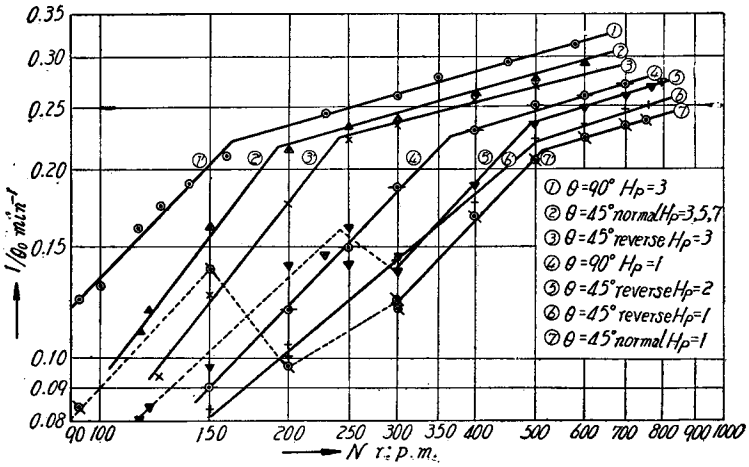

Fig. 7. Rate of solution $(1/\theta_0)$ vs agitator speed (N).
(Benzoic acid tablets in dilute NaOH solution at 15°C).

Function of Baffle Plates.

The results of agitation with and without baffle plates are shown in **Fig. 8.** Comparing curves (1) and (2) without baffles (type I) with curves (5) and (6) with baffles (type II), the former is seen to be superior in the lower range, but inferior in the higher range of agitator speeds.

It is interesting to note that the slope of curve (6) for greatest baffling is steeper than that of curve (5) with less baffling. Curve (2) in **Fig. 9** corresponds to agitation with two baffles showing a smaller slope than that of curves (5) and (6) in **Fig. 8.** Thus, when the degree of baffling is increased, vertical turbulence is increased and the slope of a curve $(1/\theta_0)$ vs N tends to be large. Curve (2) in **Fig. 9** ($n_B=2$, $w=0.15D$) corresponds to greater tangential flow, whereas curve (6) in **Fig. 8** corresponds to a pattern of vertical flow.

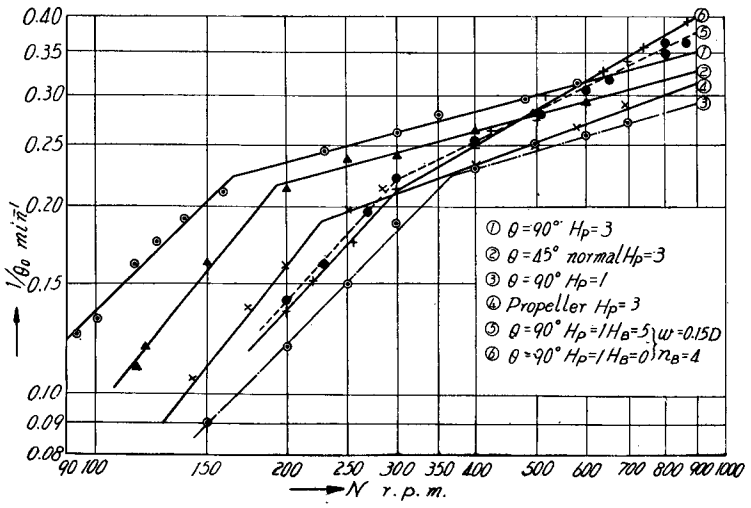

Fig. 8. Rate of solution $(1/\theta_0)$ vs agitator speed (N).
(Benzoic acid tablets in dilute NaOH solution at 15°C).

Eccentric and Inclined Installations of Agitators.

Eccentric and inclined installations of agitators are both less effective than concentric installation for solid-liquid agitation. As shown by the curves (3) and (4) in **Fig. 9,** the slope (p_2) is steeper in the case of $\varepsilon=D/4$ than in concentric agitation without baffles because of the vertical current, but the values of N_f correspond to greater agitator speed. This condition is not recommended for solid-liquid agitation.

The result of agitation by inclination of agitator shaft is shown by curve (6) of **Fig. 9.** This was measured at approximately the same conditions as in Hixson's experiment[3]. In this case, solid particles are forced into a corner of the vessel and the pattern of accumulation changes in a complex manner with increase in agitator speed. There is no definite bend in the curve of $(1/\theta_0)$ vs N corresponding to a critical agitator speed, N_f.

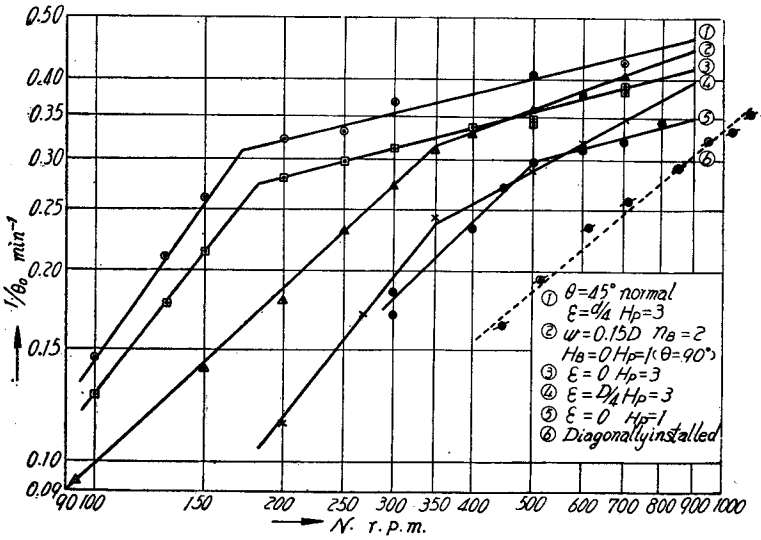

Fig. 9. Rate of solution ($1/\theta_0$) vs agitator speed (N).
(Benzoic acid tablets in dilute NaOH solution at 23°C).

e) Experimental Result, Part II (Effect of the Differences in Density between Solid and Liquid Phases).

In the case of concentric agitation without baffles, the slope of p_2 in curves of ($1/\theta_0$) vs N is nearly constant and equal to 0.28 for the benzoic acid-water system as shown in **Figs. 7,** 8 and **9.** It seems certain that the greater the difference in densities, the greater the value of p_2 as stated in section **2.** To verify this point, the authors show the effect of difference in densities with samples of benzoic acid where density differences are established by addition of copper powder (150–200 mesh) in various ratios. The conditions of preparing samples are shown in **Table 2.**

Table 2. Composition and character of tablets.

Sample number	Mixing ratio				Apparent density	Number of tablets added	Weight of one particle g.
	Benzoic acid	Copper powder	Talc	Arabic mucilage			
1	100	0	3	5	1.375	100	0.0451
2	70	30	3	5	1.77	130	0.0581
3	50	50	3	5	2.18	160	0.0715

The experimental procedures are the same as those in the case of Part I with the exception that the concentration of alkaline solution is 6.25×10^{-4} normality and the number of benzoic acid tablets is chosen as those shown in **Table 2** in the case of a vessel containing 800 c.c. (D=10 cm). Depending upon their copper content, the

number of tablets of benzoic acid added was controlled so that the times of neutralization were comparable, but the number of tablets is not necessarily arranged to be equal in effective surface area. The agitator used is also different from that used in Part I, but is coincident with that stated in **4, a.** The results of these experiments are shown in **Fig. 10.** It is clear that for larger difference in densities a larger slope p_2 is obtained as predicted from section **2.** At agitator speed greater than N_f (at 480 r.p.m.), another bend occurs. This corresponds to the agitator speed where suction of air occurs. This second agitator speed is denoted as N_a. The first critical agitator speed N_f is dependent upon the size and density of particles, whereas the second critical agitator speed N_a is dependent only upon the type of agitator and the characteristics of the liquid. The exponent in the range greater than N_a is designated as p_3. The exponents p_3 is always less than p_2 and seems to be independent of differences in density.

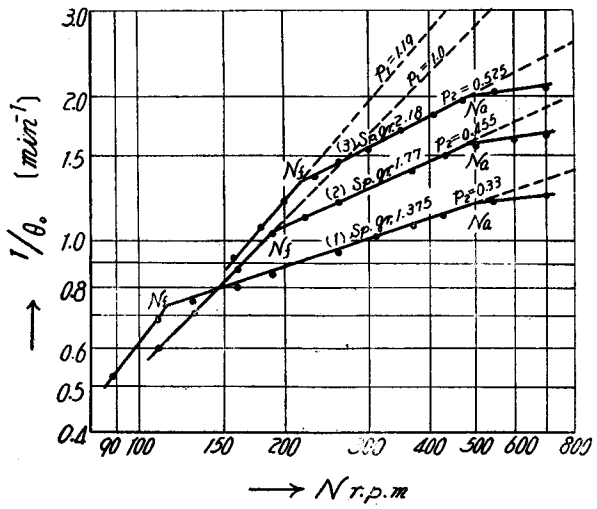

Fig. 10. Diagram showing the relation between $(1/\theta_0)$ and N for particles having various densities.
((Benzoic acid+Cu) tablets in dilute NaOH solution at 24°C)

4. Rate of Solution of Zinc Powder in Dilute Hydrochloric Acid.

As the reaction of zinc with dilute HCl,

$$Zn+2HCl \longrightarrow ZnCl_2+H_2 \qquad (10)$$

King, *et al.*[4] studied the relation between the rate of solution of a zinc cylinder with its rate of rotation in dilute HCl. They also studied the reaction mechanism and the effect of an oxidizing agent used as a depolarizer. Two steps are involved in the dissolution of Zn, that of chemical reaction and that of diffusion. The former corresponds to the reaction.

$$2H^+ \longrightarrow H_2$$

The latter is related to the diffusional velocities of HCl and $ZnCl_2$. In a series of reactions the individual reaction rate is difficult to derive, but by adding an oxi-

dizing agents such as KNO_3, resistance in the chemical reaction step can be made negligible. Thus the following reaction proceeds.

$$Zn+2HCl+KNO_3 \longrightarrow ZnCl_2+KNO_2+H_2O \tag{11}$$

In King's investigation the amount of KNO_3 added was 0.0625 mole KNO_3 per liter of solution containing 0.003 mole HCl per liter solution. In this case where the diffusional resistance is rate controlling,

$$\left.\begin{aligned} \frac{Vdc}{Sd\theta} &= K(c_s-c) \\ \frac{KS}{V} &= K' = \frac{1}{\theta}\ln\frac{c_s}{c_s-c} \end{aligned}\right\} \tag{12}$$

where $c_s=ZnCl_2$ concentration equivalent to 0.003 mole per liter HCl solution.

a) Experimental Procedure.

Agitation vessel: $D=100$ mm, $H=100$ mm,
Cylindrical vessel with flat bottom containing 800 c.c.

Agitator: $d=50$ mm, $b=15$ mm, $\theta=65°$, $H_p=4$,
made of stainless steel.

Zinc powder: (1) 80~100 mesh
(2) 100~120 mesh
(3) 120~150 mesh

The sample of zinc powder was washed with dilute NH_4Cl solution to remove ZnO that might be retained on the surface of the powder and also to make it more easily wetted. To 800 c.c. solution, 2.5 grams of zinc were added. For several conditions of experimentation, the acid concentration was selected as stated above.

After a steady state of agitation was attained, zinc powder was added and sample solution were selected at a certain intervals of time by means of a sampling apparatus, shown by **Fig. 11.** When zinc powder finer than 200 mesh was used, the experiments were difficult to perform because of difficulty of sampling.

The concentration of dissolved zinc was so low that quantitative analysis by the method of a recording polarograph was required.

As supporting electrolytes, the authors used a solution containing 1 mole of NH_4OH and 1 mole of NH_4Cl per liter. To 2.5 c.c. of the supporting electrolytic solution an equal volume of a sample solution was added. One

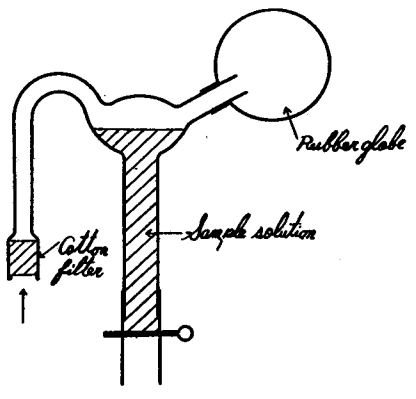

Fig. 11. Sampling apparatus.

drop of 0.5% gelatine solution was added as a maximum suppresser.

b) Experimental Results.

With reference to Eq. (12), values of $c_s/(c_s-c)$ vs θ are plotted on a semilogarithmic paper in **Fig. 12.** From the slopes of curves, specific solution rate coefficients

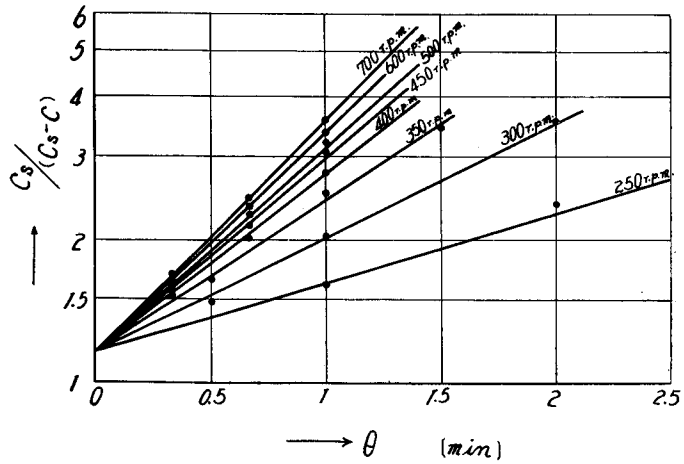

Fig. 12. Plots of $c_s/(c_s-c)$ vs θ for Zn–HCl system (10°C).

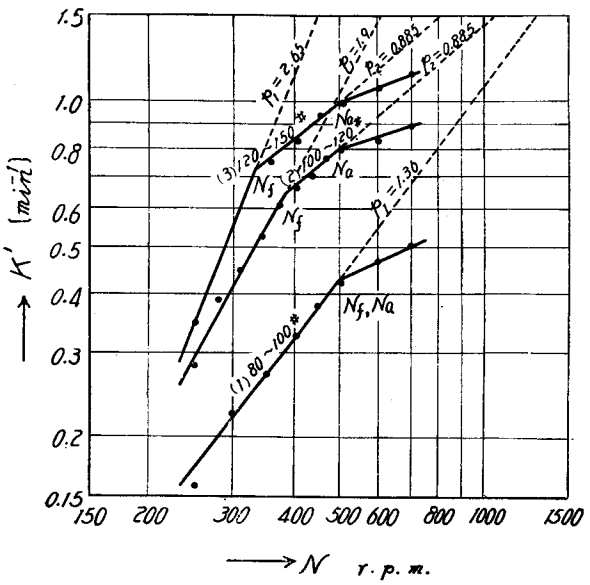

Fig. 13. Relation between K' and N for the Zn–HCl system.
(Temperature of experiments; Curve (1) 8.5°C, (2) 13°C, (3) 10°C.)

K' were obtained. In this diagram, values of $c_s/(c_s-c)$ do not approach 1.0 at $\theta=0$. This would presumably depend on either the coexistence of very fine powders or their surface condition. Values of K' were obtained for the slopes of curves in **Fig. 12,** and plotted vs agitator speed in **Fig. 13.** It can be recognized that the larger the particle size the higher the fluidization velocity N_f and the smaller the slopes for p_1, below N_f.

In the range of values above N_f, the same results were obtained as in the experiment with benzoic acid. The

specific gravity of zinc is 7.14 and of the liquid nearly 1.0 with a density difference $(\rho_s-\rho_l)$ of 6.1, and with a corresponding value of p_2, equal to 0.885. The effect of particle size upon p_2 was difficult to recognize. In the range of agitator speed greater than 480 r.p.m. (N_a), air suction due to a vortex formation takes place and the exponent p_3 assumes values less than p_2. In curve (1) for zinc powder 80~100 mesh, N_f is incidentally coincident with N_a so that there is no range corresponding to the slope p_2. At agitator speeds greater than N_f, the slope becomes equal to p_3.

5. Dissolution Rate of Magnesium Particles in Dilute Hydrochloric Acid.

The reaction of magnesium with dilute hydrochloric acid is accompanied by the evolution of hydrogen gas. To remove the hydrogen, KNO_3 was added.

a) Experimental Procedure.

The same agitator and vessel were used as with zinc.

Mg power: (1) 28~35 mesh
(2) 45~60 mesh

The magnesium powder was washed with dilute NH_4Cl solution to remove entrained MgO. A mass of 2.5 grams added to 800 c.c. of solution. The apparent density of Mg powder was found to be 1.585, whereas a value of 1.74 is reported in physical tables. This is presumably because the sample is uneven with retention of air.

A solution containing 0.003 mole of HCl and 0.0125 mole of KNO_3 per liter was used.

b) Analytical Procedure.

Since the sample solution was dilute in magnesium content as in the case of zinc, the polarographic method was used. Sample solutions were removed at a definite periods of time. For each 2.5 c.c. of sample an equal volume of another solution was added. This added solution consisted of 2.5×10^{-4} moles of ethylene diamine tetra-acetic acid and 8 moles of NH_4OH per liter of solution. One drop of 0.5% gelatine solution was added to the sample solution as a maximum suppresser. Magnesium is difficult to reduce. The half wave potential shifts so far to the negative side that basic solution is difficult to detect. This difficulty was overcome by adopting the method of R. Přibil[5] which is based upon the following reaction:

$$(\text{EDTA}-\text{Zn complex})+\text{Mg}^{++} \longrightarrow (\text{EDTA}-\text{Mg complex})+\text{Zn}^{++}$$

Thus Zn^{++} ions equivalent of Mg^{++} ions are present and the concentration of Mg^{++} is analyzed indirectly.

c) Experimental Results.

As in the case of zinc, values of $c_s/(c_s-c)$ are plotted against θ on a semilo-

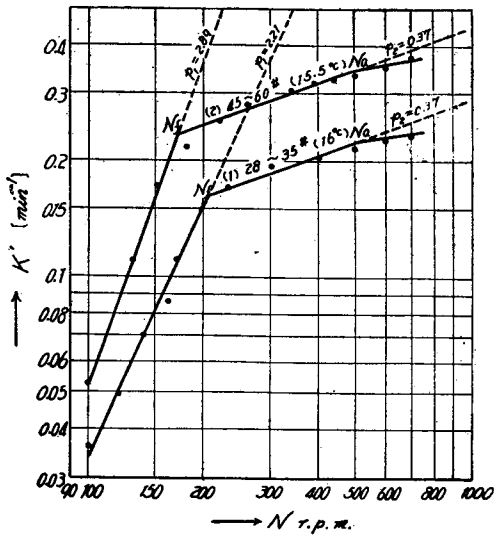

Fig. 14. Relation between K' and N for the Mg-HCl system.

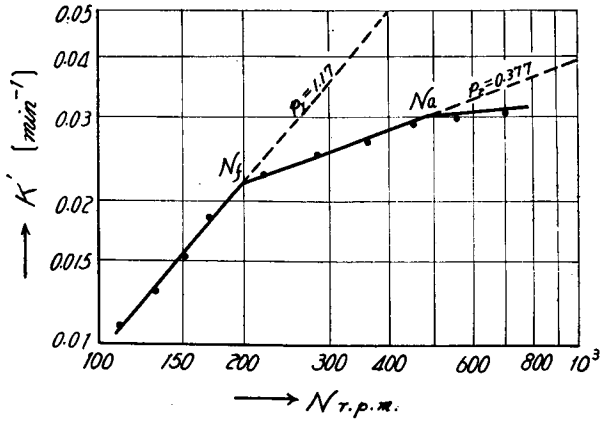

Fig. 15. Relation between K' and N for the granulated sugar-water system (19°C).

garithmic paper and the values of K' are obtained from the slopes of these curves. The correlation between K' and agitator speed N is shown in **Fig. 14.** In this diagram, two bends occur, namely at N_f and N_a.

The recognition of points corresponding to N_a is obscure. With reference to **Figs. 10** and **13,** their existence is anticipated.

In this case, the slope p_2 is equal to 0.37 and is less than for zinc. This is in agreement with the lower density of magnesium (1.585).

6. Dissolution of Cane Sugar in Water.

The rate of dissolution of cane sugar in water is so large that the shape and surface area change appreciably despite the short sampling period. The method of Ōyama and Endō[6] was adopted, namely in evaluating the limiting value of $(dc/d\theta)$ at $\theta=0$. The cane sugar crystals were common granulated sugar of average size 4 mm $\times$2 mm$\times$1.5 mm and with a specific gravity of 1.588. A mass of 20 g was added to 800 c.c. water.

For the analysis of sugar concentrations, a modified somogyi method[7] was used.

The results of experiment are shown in **Fig. 15.** The slope p_2 is equal to 0.377 nearly the same as for magnesium. The specific gravity of cane sugar is 1.588 whereas of magnesium is 1.585.

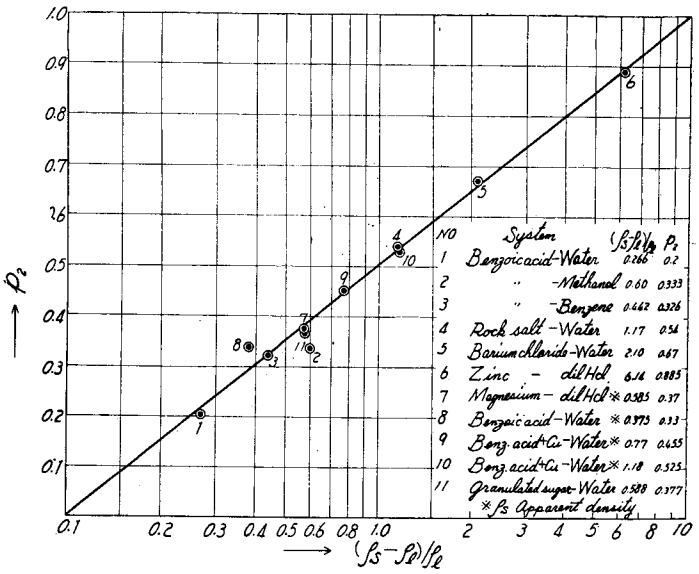

Fig. 16. Correlation of p_2 vs density difference.

7. Relation of the Exponent (p_2) to Agitator Speed in the Fluidized Range.

By summarizing the foregoing experiments, it can be concluded that the larger the difference in densities ($\rho_s-\rho_l$), the larger the exoponent (p_2) of R_e in the range of fluidization. Correlation of exponent (p_2) and $\log(\rho_s-\rho_l)/\rho_l$ is shown by a straight line in **Fig. 16.** Thus the following relation is obtained:

$$p_2 = 0.5 \log \{10(\rho_s-\rho_l)/\rho_l\} \tag{13}$$

The range of particle size of equal density and shape is so limited that their effect on p_2 is not apparent, but on a whole, it seems to be independent thereof. It is doubtful whether the relationship given by Eq. (13) can be extrapolated to particles finer than 200 mesh.

8. Three Behaviors of Solid Particles in Agitated Liquids.

The states of fluidization of solid particles in an agitated liquid are shown schematically in **Fig. 17.** This diagram shows the fluidized state for fine particles having relatively larger densities (for example zinc powder). Agitator speeds are arranged in the order of a, b and c.

In the range l_1 designated as A, solid particles gather in a pile, so that the inner surface is not effective. Another group of solid particles circulates around the center line of a cylindrical vessel forming a doughnut flow pattern, designated as type B.

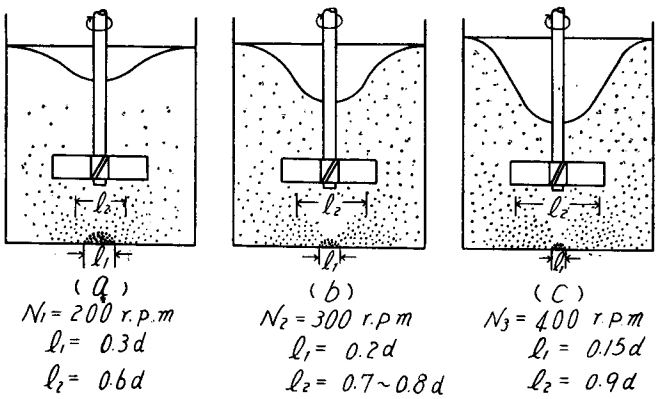

Fig. 17. Diagram showing the motion of solid particles in an agitation vessel. Zinc powder (120~150 mesh) $D = 10$ cm, $d = 0.5D$, $b = 0.15D$, $\theta = 65°$.

The diameter of the loop becomes greater with an increase in agitator speed. In this behavior the entire surface area of the particles is in similar contact with the liquid. At the higher speed N_3, l_1 tends to zero and l_2 extends to the outer end of the impeller.

With an increase in agitator speed, part of the particles may become suspended above the impeller level and then fall to the bottom of the vessel. The cycle is repeated. The group of solid particles suspended outside of the doughnut path is called group C. It is difficult to define exactly the difference between groups B and C. Solid particles corresponding to type B are subjected to three forces as follows:

$$\text{Gravity force} \sim \delta^3(\rho_s - \rho_l)g$$
$$\text{Resistance of fluid flow} \sim \delta^2 U_r^2 \rho_l \left(\sim \delta^4 n^2 \rho_l\right)$$
$$\text{Centrifugal force} \sim \delta^3(\rho_s - \rho_l) l_2 n^2 .$$

Where U_r is the relative velocity between solid particles and liquid. Under these three forces, solid particles of group B move about in a steady flow pattern, but after various periods of time they merge into group C. On the other hand solid particles of group C are accelerated by the impeller and move to the upper region of the vessel. After deceleration, they settle and shift to group A or B.

By repeating these complex motions, the particles attain a nearly steady state of motion.

The value of l_2 depends upon agitator speed, particle diameter, and the distribution ratio of particles in types B and C changes, so that Eq. (13) might be applied to particles finer than 200 mesh.

The change in states of fluidization accompanied by the increase in agitator speed for larger particles having smaller density is shown by **Fig. 18.** In this case even the tablets in the heap sometimes move about the center line of the vessel at a certain agitator speed, the difference between group A and B becomes obscure and the particles of group C are not recognized.

Rough summaries of the above results are as follows;

(1) In proportion to the increase in agitator speed, the dimension of l_2 becomes larger and that of l_1 becomes smaller and in the vicinity of agitator speed of N_f, l_1 reduces to zero.

For particles of greater density, l_1 does not always reduce to zero, but the particles of group A begin to move on the bottom surface so that the entire solid surface becomes equally accessible to the liquid. In Eq. (12), not only K but also S varies with the increase of agitator speed.

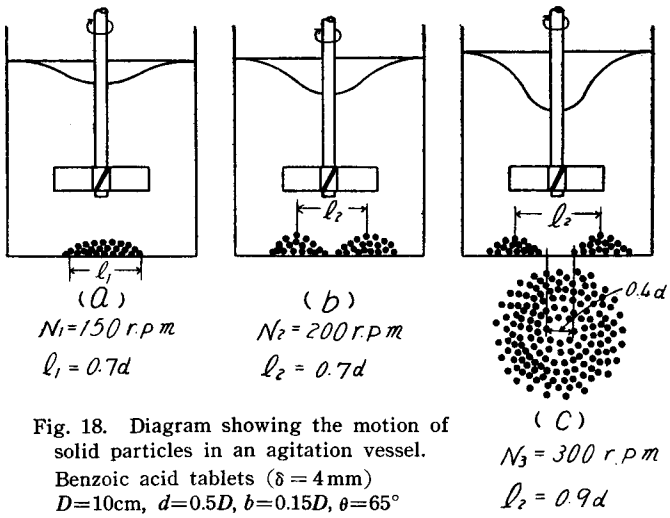

Fig. 18. Diagram showing the motion of solid particles in an agitation vessel. Benzoic acid tablets ($\delta = 4$mm) D=10cm, d=0.5D, b=0.15D, θ=65°

(2) In the range of agitator speed greater than N_f, a region void or sparse in solid particles occurs as shown in **Fig. 18c,** and the dimension l_2 remains nearly constant. In the higher range of agitator speed, particles belonging to group C predominate.

(3) For the same agitator speed l_2 is larger in the case of solid particles of smaller density and smaller diameter.

(4) In agitator speeds above N_a at which air suction due to vortex action occurs, the slope p_3 may not vary with change in particle diameter (as shown by **Fig. 13**) and with difference in densities, $(\rho_s-\rho_l)$, (as shown by **Fig. 10**). However, comparing the results over wide range of $(\rho_s-\rho_l)$, there seems to be some difference in p_3 (confer **Figs. 10** and **13**).

9. The Slope, p_1, in the Stagnant Range.

As stated above in **4. b,** the slope p_1 was greater in the case of particles of smaller size (refer to **Fig. 13**), but the effect of density was not apparent (refer to **Fig. 10**) in the range below N_f for type I.

In summary, all values of p_1 are correlated by Eq. (14) as shown by **Fig. 19.** This seems to indicate that the smaller the density and particle size, the larger the slope p_1.

$$\log \rho_s \cdot p_1 = 0.106(1/\delta) + 0.312 . \tag{14}$$

It should be noted that the ordinate values of **Figs. 10** and **13** are equal to KS/V, and that not only K but also S varies with agitator speed in this region.

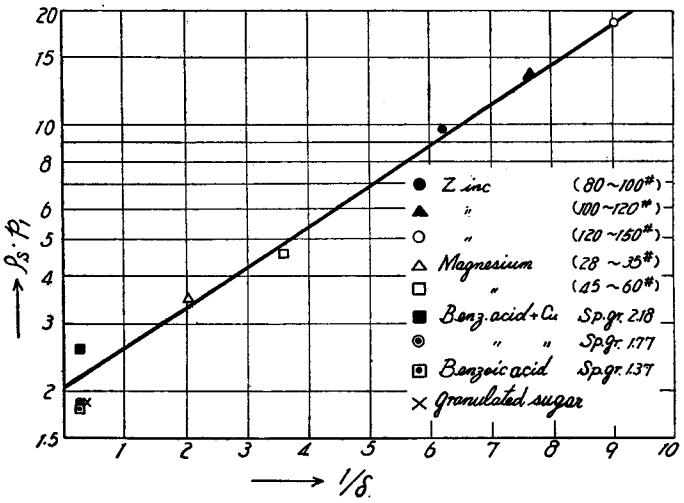

Fig. 19. Correlation of $\rho_s \cdot p_1$ vs δ.

10. Objectives of Agitation in Heterogeneous Reactions.

The principal objectives of agitation are to increase contact surface area between phases and to diminish diffusional resistance.

According to the foregoing experiments, the resistance in diffusion films decreases with increase in agitator speed where large differences in densities between the two phases occur, but this decrease becomes insignificant for smaller difference in densities.

In general greater difference in densities between phases are attainable in solid-liquid systems than in liquid-liquid systems. In solid-liquid systems, the diffusional resistance per unit area of interface diminishes rapidly with the increase in agitator speed as for example, in the case of zinc particles in dilute HCl solution, whereas with liquid-liquid systems, the diffusional resistance per unit area of interface is reduced less appreciably with the increase in agitator speed as, for example, in the case of benzoic acid in water where the difference in densities between phases is small. The effective interface between a solid and a liquid is not affected by agitation except in the stagnant range. It is concluded that the objective of agitation in the range of fluidization of solid-liquid systems is mainly to diminish diffusional resistance.

In the case of liquid-liquid systems, the degree of dispersion of droplets is increased when the agitator speed is increased so that the reaction surface area becomes larger without a corresponding change in diffusional resistance. The objective of agitation in liquid-liquid systems is chiefly to increase the interfacial area and to diminish only slightly the diffusion resistance per unit area of interface. This is the essential distinction between the objectives of agitation in solid-liquid and in liquid-liquid systems.

Acknowledgment

The authors wish to express their heartiest appreciation to Professor O. A. Hougen for his kindness in reading the original manuscript and giving many constructive suggestions and helpful criticisms. Thanks are also due to Professor S. Yoshizawa who kindly gave permission to use his polarograph equipment and to Sawamura-aen company for providing zinc powder used in this study.

Notation used.

b	: Width of impeller blades	(cm)
c	: Concentration of solution at time θ	(g/cm^3)
c_0	: Initial concentration	(g/cm^3)
c_s	: Concentration at saturation	(g/cm^3)
D	: Diameter of agitation vessel	(cm)
D_A	: Diffusion coefficient of component A (NaOH)	(cm^2/sec)
D_B	: Diffusion coefficient of component B (Benzoic acid)	(cm^2/sec)
D_f	: Diffusion coefficient of solute	(cm^2/sec)
d	: Diameter of impeller	(cm)
f_1	: A function	—
f_2	: A function	—
g	: Acceleration due to gravity	(cm/sec^2)
H	: Liquid depth	(cm)
H_B	: Elevation of baffle plate (Fig. 5)	(cm)
H_p	: Elevation of impeller above bottom (Fig. 5)	(cm)
K	: Mass transfer coefficient	(cm/sec)
$K'=(KS/V)$		(1/sec or 1/min)
l_1	: Diameter of heap of solids at rest (Fig. 17)	(cm)
l_2	: Diameter of a loop of solids (Fig. 17)	(cm)
N	: Agitator speed	(r.p.m.)
N_a	: Agitator speed at which suction of air occurs	(r.p.m.)
N_f	: Agitator speed at which fluidization of particles occurs	(r.p.m.)
n	: Agitator speed	(r.p.s.)
n_B	: Number of baffle plates	—
n_p	: Number of impeller blades	—
p	: Exponent of Reynolds number	—
p_1	: Exponent of R_e or N in stagnant range	—
p_2	: Exponent of R_e or N in fluidized range	—
p_3	: Exponent of R_e or N in suction range	—
q	: Exponent of Schmidt number	—

$R_e=\frac{D^2n\rho_l}{\mu}$	=Reynolds number	—
R_f	: Critical Reynolds number at which fluidization occurs	—
r	: Exponent of the term (δ^3g/ν^2)	—
s	: Exponent of the term (δ/D)	—
S	: Surface area of solid particles	(cm^2)
t	: Exponent of the term $(\rho_s-\rho_l)/\rho_l$	—
V	: Total volume of solution	(cm^3)
W	: Weight of solid particle	(mole)
w	: Width of baffle plates	(cm)
x	: Thickness of diffusion film	(cm)
x_1	: Thickness of diffusion layer from the surface of solid to the plane where neutralization occurs (Fig. 4)	(cm)
$\alpha, \alpha', \alpha''$	: Proportionality constant	—
δ	: Particle diameter	(cm)
ε	: Eccentric distance of an agitator shaft	(cm)
ρ_l	: Density of agitated liquid	(g/cm^3)
ρ_s	: Density of solid particles	(g/cm^3)
θ	: Time elapsed from interfacial contact	(sec, min)
θ_0	: Time required for neutralization	(min)
θ	: Angle of impeller blades (refer to Fig. 5)	—
μ	: Viscosity of agitated liquid	(g/cm·sec)
$\nu=\mu/\rho_l$	: Kinematic viscosity of liquid	(cm^2/sec)

Literature cited

1) A. W. Hixson and S. J. Baum, Ind. Eng. Chem., **33**, 478 (1941).
2) D. E. Mack and R. A. Marriner, Chem. Eng. Progr., **45**, 545 (1949).
3) A. W. Hixson and S. J. Baum, Ind. Eng. Chem., **34**, 120 (1942).
4) C. V. King and M. Schack, J. A. Ch. S., **54**, 1744 (1932); **57**, 1213 (1935).
5) R. Přibil and Z. Roubal, Collection Czechoslov Chem. Commun., **19**, 252 (1954).
6) Y. Ōyama and K. Endō, Chem. Eng. (Japan), **20**, 576 (1956).
7) T. Kobayashi, et al, Journ. of Agricul. Chem. Soc. of Japan, **28**, 171 (1954).